

Direct Observation of Dynamical Switching between Two Driven Oscillation States of a Josephson Junction.

I. Siddiqi, R. Vijay, F. Pierre, C.M. Wilson, L. Frunzio, M. Metcalfe, C. Rigetti, R.J. Schoelkopf, and M.H. Devoret
Departments of Applied Physics and Physics, Yale University, New Haven, Connecticut 06520-8284

D. Vion and D. Esteve

Service de Physique de l'Etat Condensé, CEA-Saclay, F-91191 Gif-sur-Yvette (France)

(Received textdate; Revised textdate; Accepted textdate; Published textdate)

We performed a novel phase sensitive microwave reflection experiment which directly probes the dynamics of the Josephson plasma resonance in both the linear and non-linear regime. When the junction was driven below the plasma frequency into the non-linear regime, we observed for the first time the transition between two different dynamical states predicted for non-linear systems. In our experiment, this transition appears as an abrupt change in the reflected signal phase at a critical excitation power.

As first understood by Josephson, a superconducting tunnel junction can be viewed as a non-linear electrodynamic oscillator [1]. The tunneling of Cooper pairs manifests itself as a non-linear inductance that shunts the linear junction self-capacitance C_J , formed by the junction electrodes and the tunnel oxide layer. The constitutive relation of the non-linear inductor can be written as $I(t) = I_0 \sin \delta(t)$, where $I(t)$, $\delta(t) = \int_{-\infty}^t dt' V(t') / \varphi_0$ and $V(t)$ are the current, gauge-invariant phase-difference and voltage corresponding to the inductor, respectively, while the parameter I_0 is the junction critical current. Here $\varphi_0 = \hbar/2e$ is the reduced flux quantum. For small oscillation amplitude, the frequency of oscillation is given for zero bias current by the so-called plasma frequency $\omega_P = 1/\sqrt{L_J C_J}$ where $L_J = \varphi_0/I_0$ is the effective junction inductance. As the oscillation amplitude increases, the oscillation frequency decreases, an effect which has been measured in both the classical and quantum regime [2, 3, 4, 5, 6, 7]. However, a more dramatic non-linear effect should manifest itself if the junction is driven with an AC current $i \sin \omega t$ at a frequency ω slightly below ω_P . If the quality factor $Q = C_J \omega_P / \text{Re}[Z^{-1}(\omega_P)]$ is greater than $\sqrt{3}/2\alpha$, where $Z(\omega_P)$ is impedance of the junction electrodynamic environment and $\alpha = 1 - \omega/\omega_P$ the detuning parameter, then the junction should switch from one dynamical oscillation state to another when i is ramped above a critical value i_{c1} [8]. For $i < i_{c1}$, the oscillation state would be low-amplitude and phase-lagging while for $i > i_{c1}$, the oscillation state would be high-amplitude and phase-leading. This generic non-linear phenomenon, which we refer to as “dynamical switching”, is reminiscent of the usual “static switching” of the junction from the zero-voltage state to the voltage state when the DC current bias exceeds the critical current I_0 [9]. However, an important distinction between dynamical and static switching is that in dynamical switching, the phase particle remains confined to only one well of the junction cosine potential $U(\delta) = -\varphi_0 I_0 \cos(\delta)$, and the time-average value of δ is always zero. The junction never switches to the “normal” state, and thus no DC voltage is generated. Also,

for dynamical switching, the current i_{c1} depends both on Q and on the detuning α . In this Letter we report the first direct observation of this dynamical switching effect in a Josephson junction. The parallel with static switching suggests that dynamical switching can be used for amplification with the added advantage that no energy dissipation occurs in the junction chip, a desirable feature for the readout of superconducting qubits [10].

Typical junction fabrication parameters limit the plasma frequency to the 20 - 100 GHz range where techniques for addressing junction dynamics are inconvenient. We have chosen to shunt the junction by a capacitive admittance to lower the plasma frequency by more than an order of magnitude and attain a frequency in 1-2 GHz range (microwave L-band). In this frequency range, a simple on-chip electrodynamic environment with minimum parasitic elements can be implemented, and the hardware for precise signal generation and processing is readily available. In our experiment, we directly measure the plasma resonance in a coherent microwave reflection measurement. Unlike previous experiments which measured only the microwave power absorption at the plasma resonance [2, 3, 7], we also measure the phase ϕ of the reflected microwave signal. Thus, we can detect the characteristic signature of the transition between different oscillating states of the junction – a change of oscillation phase relative to the drive. Note that the phase ϕ of the reflected signal which probes the phase of the oscillation state should not be confused with the junction gauge-invariant phase difference δ .

In the first step of sample fabrication, a metallic underlayer – either a normal metal (Au, Cu) or a superconductor (Nb) – was deposited on a silicon substrate to form one plate of the shunting capacitor, followed by the deposition of an insulating Si_3N_4 layer. Using e-beam lithography and double-angle shadow mask evaporation, we subsequently fabricated the top capacitor plates along with a micron sized $\text{Al}/\text{Al}_2\text{O}_3/\text{Al}$ tunnel junction. The critical current of the junction was in the range $I_0 = 1 - 2 \mu\text{A}$. By varying both the dielectric layer thickness and the pad area, the capacitance C was varied between

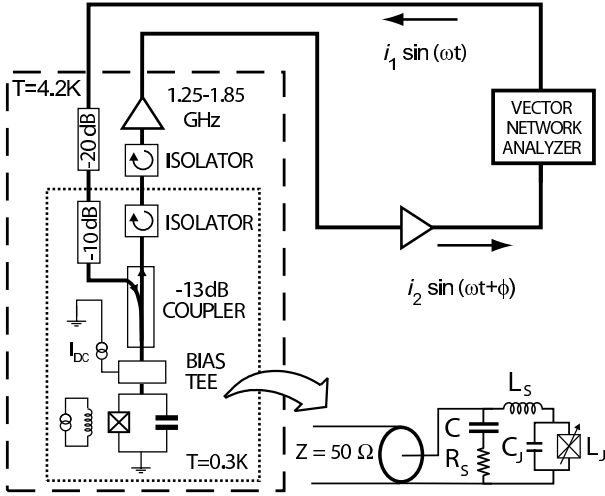


FIG. 1: Schematic of the measurement setup. Thick lines correspond to 50Ω coaxial transmission lines. A lumped element model for the junction chip and measurement line is shown. The two ideal current sources actually represent external sources.

16 and 40 pF. Sample parameters are listed in Table I.

The junction + capacitor chip is placed on a microwave circuit-board and is wire-bonded to end of a coplanar stripline which is soldered to a coaxial launcher affixed to the side wall of the copper sample box. We anchor the RF leak-tight sample box to the cold stage of a ^3He refrigerator with base temperature $T = 280$ mK. The measurement setup is schematically shown in Figure 1. Microwave excitation signals are generated by a HP 8722D vector network analyzer and coupled to the sample via the -13 dB side port of a directional coupler. The reflected microwave signal passes through the direct port of the coupler, and is amplified first using a cryogenic 1.20 – 1.85 GHz HEMT amplifier with noise temperature $T_N = 4$ K before returning to the network analyzer. A DC bias current can be applied to the junction by way of a bias tee. We use cryogenic attenuators and isolators on the microwave lines in addition to copper-powder and other passive filters [5] on the DC lines to shield the junction from spurious electromagnetic noise.

We locate the linear plasma resonance by sweeping the excitation frequency from 1 to 2 GHz and measuring the reflection coefficient $\Gamma(\omega) = i_2/i_1 e^{j\phi} = (Z(\omega) - Z_0)/(Z(\omega) + Z_0)$, where $Z_0 = 50\Omega$ is the characteristic impedance of our transmission lines and $Z(\omega)$ is the impedance presented to the analyzer by the chip and the measurement lines. For an ideal LC resonator without intrinsic dissipation, we expect a phase shift $\Delta\phi = \phi_{\omega \gg \omega_p} - \phi_{\omega \ll \omega_p} = 2\pi$, which we verified by placing a chip capacitor and an inductive wire bond in place of the junction chip. An important aspect of our experiment is that Q is now determined by the ratio $Z_0/Z_J \sim 10$, where $Z_J = \sqrt{L_J/(C_J + C)}$ and not by the intrinsic junction losses which are negligible. An excitation power $P = i^2 Z_0/4 \approx -120$ dBm (1 fW) corresponding to a cur-

Sample	L_J (nH)	$\omega_p/2\pi$ (GHz)	C (pF)	L_S (nH)
1	0.28	1.18	39 ± 1	$0.20 \pm .02$
2	0.18	1.25	30 ± 4	$0.34 \pm .04$
2a	0.17	1.66	18 ± 1	$0.32 \pm .02$
3	0.32	1.64	16 ± 1	$0.27 \pm .02$
4	0.38	1.81	19 ± 1	$0.026 \pm .02$
5	0.40	1.54	19 ± 1	$0.15 \pm .02$

TABLE I: Sample parameters. $L_J = \varphi_0/I_0$ and ω_p are measured values. C and L_S are fit values to the data. Samples 1,2 and 2a have a 100 nm thick Au underlayer, sample 3 has a 50 nm thick Nb underlayer, sample 4 has a $1\mu\text{m}$ thick Cu underlayer, and sample 5 has a 200 nm thick Nb underlayer.

rent $i = 9\text{ nA} \ll I_0$ keeps the junction in the linear regime.

In Figure 2, we present the reflected signal phase ϕ as a function of excitation frequency for sample 5. In order to remove the linear phase evolution associated with the finite length of the measurement lines, we have subtracted from our measurement in the superconducting state the reflection coefficient measured with the junction in the normal state. The point where $\phi = 0$ is the linear-regime plasma frequency. For sample 5, $\omega_p/2\pi = 1.54$ GHz.

The precise frequency and critical current dependence of the reflected signal phase of our samples can be accounted for by a 3-element model for the electrodynamic environment seen by the junction. This lumped element model is shown in the lower right corner of Figure 1. The parasitic inductance L_S and resistance R_S model the non-ideality of the shunting capacitor C . They arise from the imperfect screening of currents flowing in the capacitor plates and the finite conductivity of these

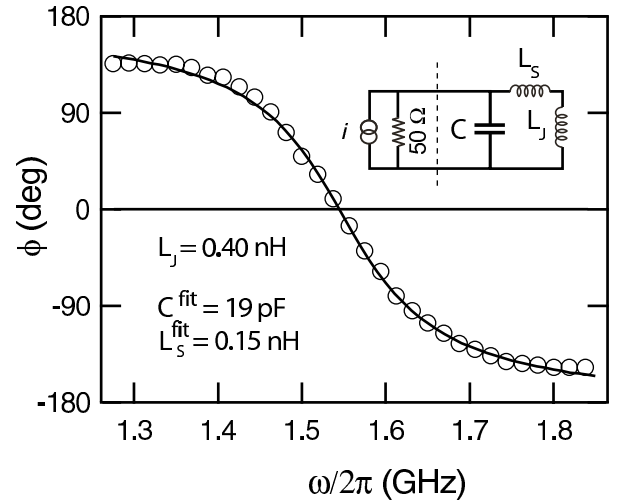


FIG. 2: Normalized reflected signal phase ϕ as a function of excitation frequency for sample 5. The open circles are measured data for $L_J = 0.40$ nH. The solid line is calculated from the equivalent circuit model shown in the inset. The magnitude of the reflected signal is unity.

plates. The plasma frequency in the linear regime is determined by the total inductance $L_J + L_S$ and capacitance $C_{eff} = C_J + C \simeq C$, and is given by the following relation:

$$\left(\frac{1}{\omega_p}\right)^2 = C(L_J + L_S) = \frac{\varphi_0 C}{I_0} + CL_S.$$

We thus plot $1/\omega_p^2$ versus $1/I_0 = L_J/\varphi_0$ in Figure 3 for samples 1, 2, 4 and 5. As the critical current is decreased by applying a magnetic field, the junction inductance increases, and the plasma frequency is reduced. For each sample, a linear fit to the data yields the values of C and L_S . The fit values for C agree well with simple estimates made from the sample geometry. Samples 1 and 2 have nominally the same capacitance but different critical current, and hence lie approximately on the same line in Figure 3. A total of four capacitive pads were used to make the shunting capacitor in samples 1 and 2, and after initial measurements, we scratched off two of the pads from sample 2 to obtain sample 2a. The fit parameters for sample 2a indicate that the capacitance is indeed halved. For samples with a thin underlayer (1,2 and 3), a stray inductance in the range $L_S = 0.20 - 0.34$ nH is observed. For samples 4 and 5 with a significantly thicker underlayer, L_S was reduced to 0.026 nH and 0.15 nH respectively. This behavior is consistent with the calculated screening properties of our thin films. To verify that the values of C and L_S were not affected by the magnetic field used to vary I_0 , we varied L_J by applying a DC bias current [7] at zero magnetic field. The resonance data obtained by this method agrees with the magnetic field data. With a single set of parameters, we can accurately fit both the position of the resonance and its lineshape. Additionally, we find $R_S = 0.8 \Omega$ for samples 1 and 2, $R_S = 0.02 \Omega$ for sample 4, and $R_S = 0$ for the superconducting samples 3 and 5. The fit for sample 5 is shown as a solid line in Figure 2. Finally, we have independently verified the effect of the shunting capacitor on the plasma resonance by performing resonant activation experiments [4].

In order to study the non-linear regime of the plasma resonance, we measured the reflection coefficient as a function of frequency for increasing power. We present the data for sample 5 as a two dimensional color plot in the lower panel of Figure 4 in which each row is a single frequency sweep, similar to Figure 2. For small excitation power, we recover the linear plasma resonance at 1.54 GHz, shown as a yellow line corresponding to $\phi = 0$. As the power is increased above -115 dBm, the plasma frequency decreases, as is expected for a junction driven with large amplitude [4]. The boundary between the leading-phase region (green) and the lagging-phase region (red) therefore curves for high powers. This curvature has an interesting consequence: When we increase the drive power at a constant frequency slightly below the plasma frequency, the phase as a function of power undergoes an abrupt step, as predicted [8]. For yet greater powers (> -90 dBm), we encounter a new

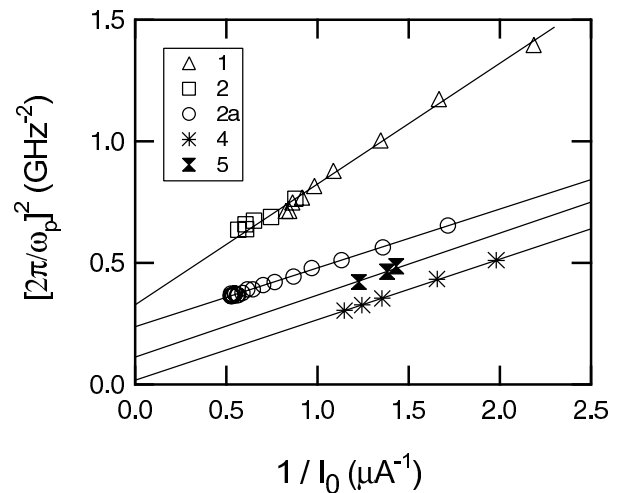


FIG. 3: Inverse square of the plasma frequency $1/\omega_p^2$ as a function of the inverse critical current $1/I_0 = L_J/\varphi_0$ for samples 1,2,4 and 5. Solid lines are linear fits to the data corresponding to the model of Fig. 1, with a single best fit line drawn for samples 1 and 2 which nominally differ only in I_0 .

dynamical regime (black region in Figure 4) where δ appears to diffuse between the wells of the cosine potential. When measuring the AC junction resistance at $f = 221$ Hz in presence of the microwave drive, a finite resistance was only observed in the black region. To verify that this phenomenon was not due to junction heating, we have varied the ramp time of the power and no change in the transition power was observed. In the lower panel of Figure 4, we illustrate the sequence of dynamical transitions by plotting ϕ as a function of incident power at $\omega/2\pi = 1.375$ GHz. For $P < -102$ dBm, the phase is independent of power (δ oscillates in a single well in the harmonic-like, phase-leading state, letter A). For -102 dBm $< P < -90$ dBm, the phase evolves with power and δ still remains within the same well, but oscillates in the anharmonic phase-lagging state (letter B). Finally, for $P > -90$ dBm, the average phase of the reflected signal saturates to -180 degrees, corresponding to a capacitive short circuit (letter C). This last value is expected if δ hops randomly between wells, the effect of which is to neutralize the Josephson inductive admittance.

The value of the switching current i_{c1} for the A-B transition, which is a function of both the detuning α and power P , is in good qualitative agreement with the analytical theory which retains only the first anharmonic term in the cosine potential [8]. For instance, the slope of the A-B transition line at the linecut in Figure 4, $dP(\text{dBm})/d\alpha(\%) = 0.8$ for the experiment while we calculate its value to be 0.7. Furthermore, in measurements in which the power is ramped in less than 100 ns, we verified that the transition between dynamical states is hysteretic, another prediction of the theory. These results will be presented in a later publication. To explain the complete frequency and power dependence of the transi-

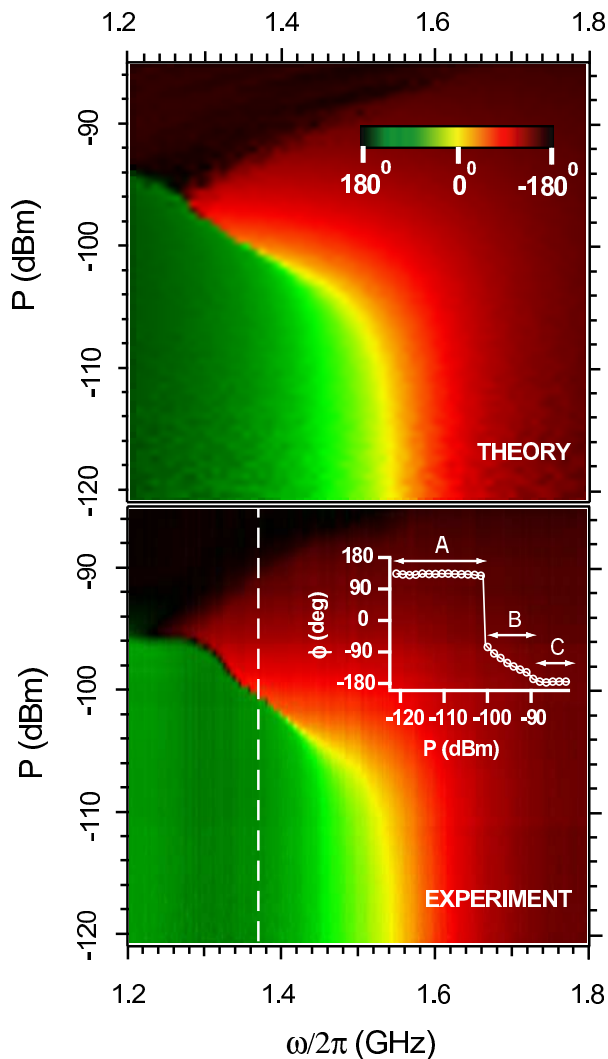


FIG. 4: Normalized reflected signal phase ϕ (wrap-around color scheme) as a function of excitation frequency $\omega/2\pi$ and excitation power P . In the lower panel, a vertical slice taken at $\omega/2\pi = 1.375$ GHz (dashed line) shows the abrupt transition between two oscillation states of the system. The upper panel is the result of numerical simulations.

tions shown in the lower panel of Figure 4, we have performed numerical simulations by solving the full circuit model of the lower corner of Figure 1, including the exact junction non-linear constitutive relation. The result of this calculation is shown in the upper panel of Figure 4. It correctly predicts the variation of the plasma frequency with excitation power, and the boundaries of the phase diffusion region. The agreement between theory and experiment is remarkable in view of the simplicity of the model used with no adjustable parameters, and only small differences in exact shape of region boundaries are observed. It is important to mention that the overall topology of Figure 4 is unaffected by changes in the parameter values within the bounds of Table I.

In conclusion, we have performed a novel, phase-sensitive, microwave experiment demonstrating that the Josephson plasma oscillation can switch between the two dynamical states predicted for a driven non-linear system. At the critical excitation power we observe an abrupt change in the reflected signal phase. In accordance with the analytical theory and numerical simulations, we have observed that this critical power is a strong function of the junction critical current. This phenomenon can therefore be applied to the detection of small relative variations in critical current in the same manner that the usual DC SQUID, biased in the vicinity of the critical current, transforms a flux-induced variation in critical current into a DC voltage [11]. Furthermore, following the methodology invented for experiments with trapped electron systems [12], we can use this dynamical switching as the basis for a single-shot and latching qubit readout. Since the measurement of phase is purely dispersive, this new readout would have advantage the of eliminating dissipation at the chip level, a limiting factor for superconducting qubits.

We would like to thank D. Prober for use of his laboratory equipment and useful discussions, Abdel Aassime for help in the initial sample fabrication, and L. Grober for assistance with the electron microscope. This work was supported by the ARDA (ARO Grant DAAD19-02-1-0044) and the NSF (Grant DMR-0072022).

-
- [1] B. Josephson, *Rev. Mod. Phys.* 36, 216 (1964).
 - [2] A.J. Dahm, A. Denenstien, T.F. Finnegan, D.N. Langenberg, and D.J. Scalapino, *Phys. Rev. Lett.* 20, 859 (1968).
 - [3] J. Mygind, N.F. Pedersen, and O.H. Soerensen, *Appl. Phys. Lett* 29, 317 (1976).
 - [4] M.H. Devoret, D. Esteve, J.M. Martinis, A. Cleland, and J. Clarke, *Phys. Rev. B* 36, 58 (1987).
 - [5] J.M. Martinis, M.H. Devoret, and J. Clarke, *Phys. Rev. B* 35, 4682 (1987).
 - [6] B. Yurke, L.R. Corruccini, P.G. Kaminsky, L.W. Rupp, A.D. Smith, A.H. Silver, R.W. Simon, and E.A. Whittaker, *Phys. Rev. A* 39, 2519 (1989).
 - [7] T. Holst and J. Bindslev Hansen, *Physica B* 165-166, 1649 (1990).
 - [8] M.I. Dykman and V.N. Smelyanski, *Phys. Rev. A* 41, 3090 (1990).
 - [9] T.A. Fulton and L.N. Dunkleberger, *Phys. Rev. B* 9, 4760 (1974).
 - [10] D. Vion, A. Aassime, A. Cottet, P. Joyez, H. Pothier, C. Urbina, D. Esteve, and M. Devoret, *Science* 296, 886 (2002).
 - [11] S.T. Ruggiero and D.A. Rudman (eds.), Chap 2. by J. Clarke "SQUIDS: Principles, Noise, and Applications", *Superconducting Samples*, Academic Press, San Diego (1990).
 - [12] C.H. Tseng, D. Enzer, G. Gabrielse, and F.L. Walls, *Phys. Rev. A* 59, 2094 (1999).